Dual-targeted and MRI-guided photothermal therapy via iron-based nanoparticles-incorporated neutrophils

Note – this file has been updated and corrected when compared to the version originally published on 19th February 2021.

Jing Wang,[†a] Tianxiao Mei,[†a] Yang Liu,[a] Yifan Zhang,[a] Ziliang Zhang,[a] Yihui Hu,[a] Yibin Wang,[b] Minliang Wu,[c] Chuanxue Yang,[a] Xiangdong Zhong,[a] Bingdi Chen,[*a] Zheng Cui,[d] Wenjun Le,[*a] and Zhongmin Liu,[*a]

a. Institute for Regenerative Medicine, Shanghai East Hospital, The Institute for Biomedical Engineering & Nano Science, School of Medicine & School of Life Sciences and Technology, Tongji University, Shanghai 200092, China
b. Department of Radiology, Shanghai East Hospital, Tongji University School of Medicine, Shanghai 200092, China
c. Department of Plastic Surgery, Changhai Hospital, Second Military Medical University, Shanghai 200433, China
d. Departments of Pathology, Wake Forest University School of Medicine, Winston-Salem, NC 27157, USA

[†]These Authors contributed equally to this work.

*Corresponding Author:

Wenjun Le, wenjunle@tongji.edu.cn

Bingdi Chen, inanochen@tongji.edu.cn

Zhongmin Liu, liu.zhongmin@tongji.edu.c

Supplementary Materials and Methods

Materials

All initial reagents were commercially available. Iron (III) chloride hydrate ($FeCl_3$•$6H_2O$), ethylene glycol, sodium acetate, ammonium hydroxide (NH_4OH, 28 wt%), and hydrochloric acid (37 wt% aqueous solution) were purchased from Shanghai (China) Reagent Company. Tetraethyl orthosilicate (TEOS), (3-Aminopropyl) triethoxysilane (APTES), and fluorescein isothiocyanate (FITC) were obtained from Sigma-Aldrich (USA). Dulbecco's Modified Eagle's Medium (DMEM), fetal bovine serum (FBS), and Dulbecco's phosphate buffered saline (PBS) were obtain from Biological Industries (Israel). hematoxylin and eosin (H&E) was obtained from Beyotime (China). Percoll was obtained from GE Healthcare (USA).

Instruments

Transmission Electron Microscopy images were obtained by a Philips Tecnai 20 microscope (Philips, Netherlands). The hydrodynamic diameter and the zeta potentials of the nanoparticles were obtained on a Dynamic light scattering particle size analyzer (Zetasizer Nano-ZS90, Malvern, UK). The photothermal effect was tested on an 808 nm laser (Beijing Energylaser Tech. Ltd., China). Temperature changes and thermal images were monitored and taken by an IR thermal camera (DALI Technology). The absorbance at 450 nm for CCK-8 assay, the fluoresce intensity and the UV-vis absorption spectra were measured using a multifunction microplate reader (Infinite M200 Pro, Switzerland). The MRI experiments were performed on a clinical MRI instrument (GE Discovery 750W 3.0T, USA). The iron concentration per gram in tumor tissue was measured by ICP-OES (Agilent 725 ICP-OES, USA)

Cell culture

Mouse Pancreatic cells (Pan02, 3111C0001CCC000446) were purchased from the National Infrastructure of Cell Line Resource (China). Pan02 cells were grown in DMEM medium containing 10% FBS and 1% penicillin-streptomycin at 37°C in a 5% CO_2 humidified atmosphere.

Establishment of Pan02-small animal models.

All the mice were allowed free access to food and water. All animal experiments were conducted in compliance with the guidelines outlined in the National Institute of Health Guide for the Care and Use of Laboratory Animals. The C57BL/6 mice were injected s.c. at the right flank close to leg with 5×10^6 Pan02 cells.

ICP-OES

Pan02 tumor xenograft C57BL/6 mouse models with a tumor volume of 50 mm^3 were intravenously injected by 200 μL NSNP or NSNP@Ne (at a dose of 200 μg NSNP). The iron contents in tumors were measured with ICP-OES.

Calculation of photothermal conversion efficiency

The photothermal conversion efficiency (η) was calculated using the following equation:

$$\eta = \frac{hS(T_{max} - T_{surr}) - Q_{dis}}{I(1 - 10^{-A_{808}})}$$

In this equation, h is the coefficient of heat transfer, S is the surface area, T_{max} is the equilibrium temperature and T_{surr} is the ambient temperature of the surroundings. Q_{dis} denotes the heat absorbed by water, I is the 808 nm laser power density, and A_{808} is the optical density of NSNP at the wavelength of 808 nm. The data of S, Tmax, Tsurr, I, and A808 nm can be obtained by direct measurement. However, the data of h and Qdis were calculated according to the specific implementation of the photothermal performance test experiment. the following equation is used to determine the hS:

$$hS = \frac{\Sigma_i m_i c_{p,i}}{\tau_s} \approx \frac{cm}{\tau_s}$$

where, m and c are the weight and specific heat capacity of solvent (water), respectively, while, τs is the heat dissipation time constant. Whereas, τs is calculated by plotting a linear data of cooling

period with the negative natural logarithm using the following equation:

$$t = -\tau_s In \frac{T - T_{surr}}{T_{max} - T_{surr}} = -\tau_s In\theta$$

Q_{dis} represents the heat emitted by the solvent absorbing the 808 nm laser, measured by a control experiment of water. Qdis was calculated using the following equation:

$$Q_{dis} = cm\Delta T_{H_2O}$$

In vivo photothermal efficiency

Pan02 tumor xenograft C57BL/6 mouse models with a tumor volume of 50 mm^3 were intravenously injected by Saline, NSNP@Ne (10 mg/kg NSNP with 5×10^5 autologous neutrophils/kg). The tumor areas were exposed to 808 nm laser irradiation at a power density of 3 W/cm^2 or 1 W/cm^2, and the temperature was recorded in 10 min. 24 h after irradiation, the mice were sacrificed and the tumor tissue was collected for H&E staining.

Supplementary Figures

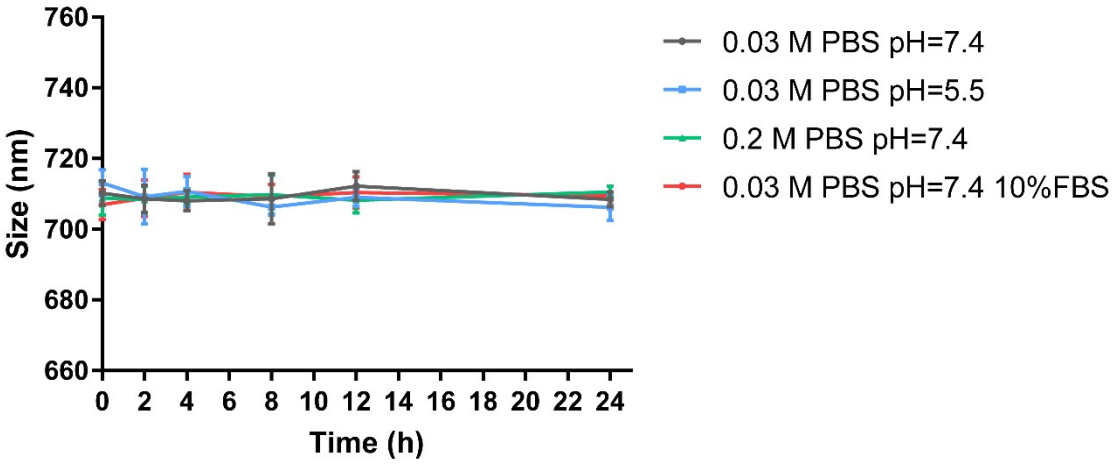

Fig. S1 Stability of NSNP in different media (0.03 M PBS at pH 7.4, 0.03 M PBS at pH 5.5, 0.2 M PBS at pH 7.4, and 0.03 M PBS at pH 7.4 plus 10% FBS). Data represents the mean ± SD (n=3).

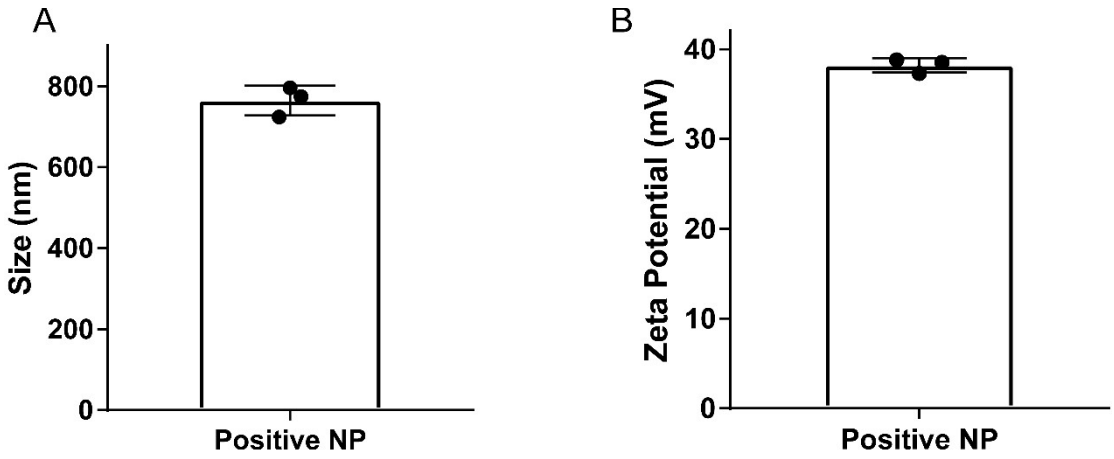

Fig. S2 (A) Hydrodynamic diameters and (B) zeta potentials of Positive NP. Data represent the mean ± SD (n=3)

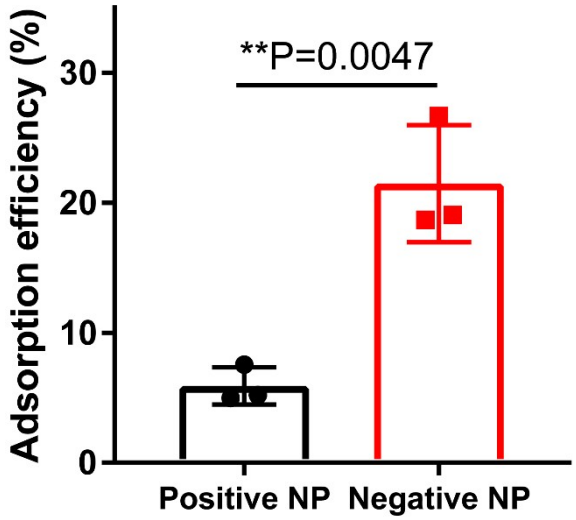

Fig. S3 Absorption efficiency towards neutrophils of nanoparticles with different surface charges. Statistical significance was calculated via a Student's t-test. $^{*}P < 0.05$; $^{**}P < 0.01$; $^{***}P < 0.001$; and $^{****}P < 0.0001$.

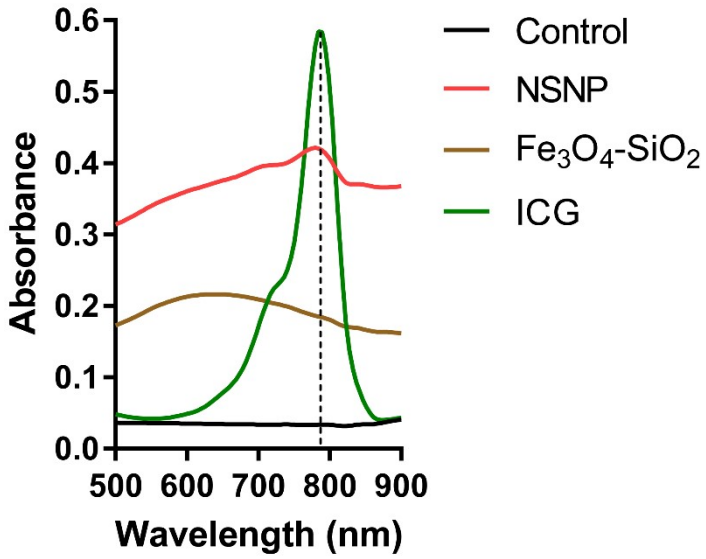

Fig. S4 UV-vis absorption spectra of Control (black), NSNP (red), Fe_3O_4-SiO_2 (brown), and ICG (green).

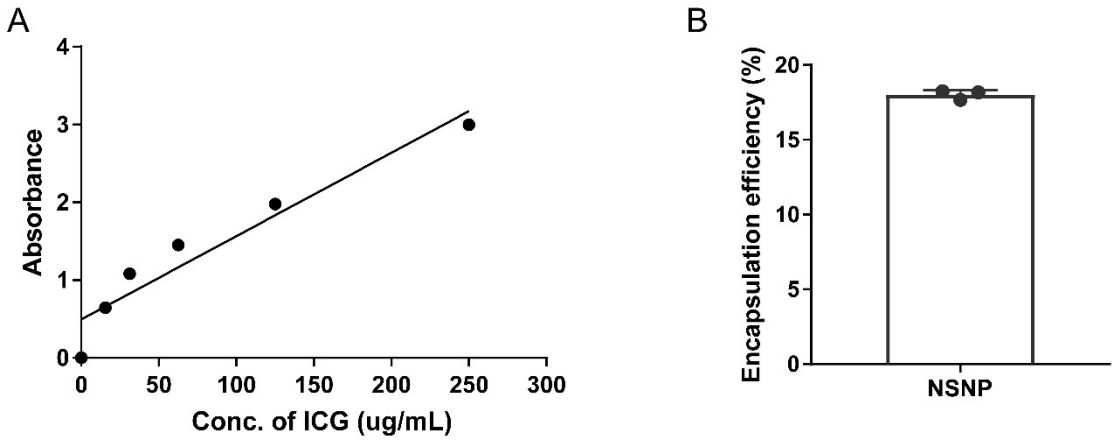

Fig. S5 (A) The standard curve of UV absorption towards ICG concentration. (B) The encapsulation efficiency of ICG in NSNP. Data in B represents the mean ± SD (n=3).

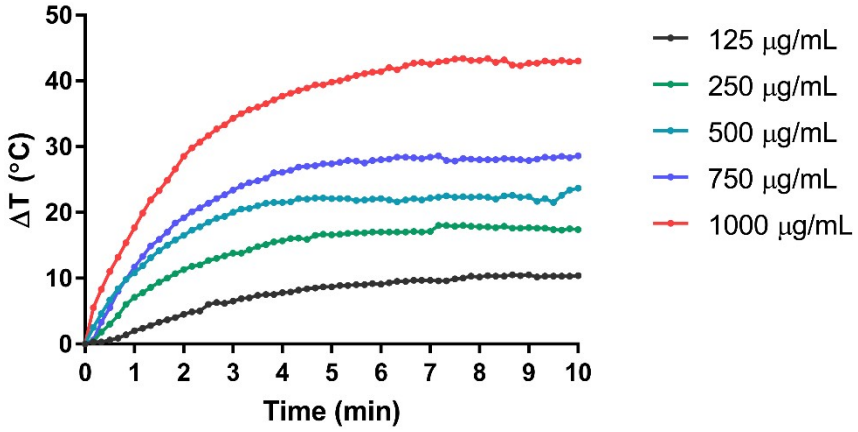

Fig. S6 Temperature rising curve of NSNP at different concentrations from 0.125 to 1 mg/mL with 808 nm laser irradiation (3 W/cm^2, 10 min).

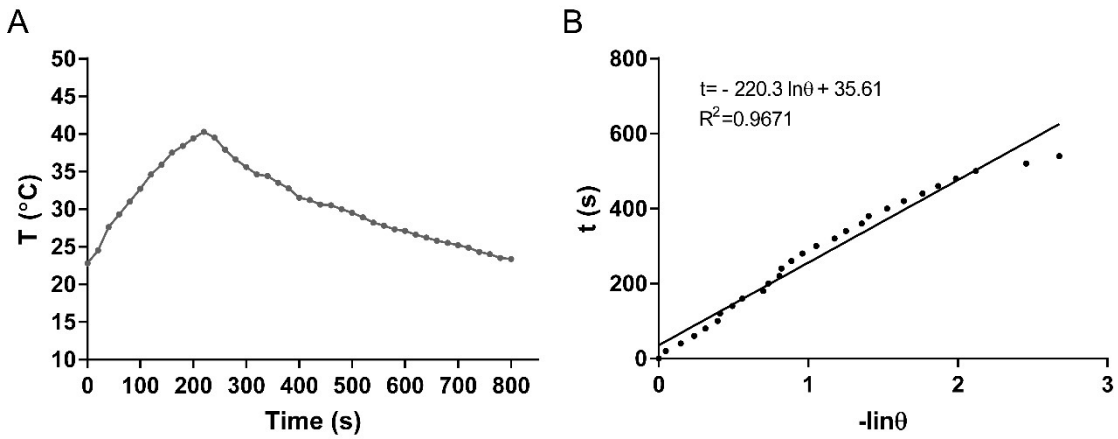

Fig. S7 Data for photothermal conversion efficiency. (A) Temperature change curve of NSNP aqueous solution after illumination of 808 nm laser (2 W/cm^2) to maximum temperature and by naturally cooling. (B) The plot of time against temperature during the cooling period.

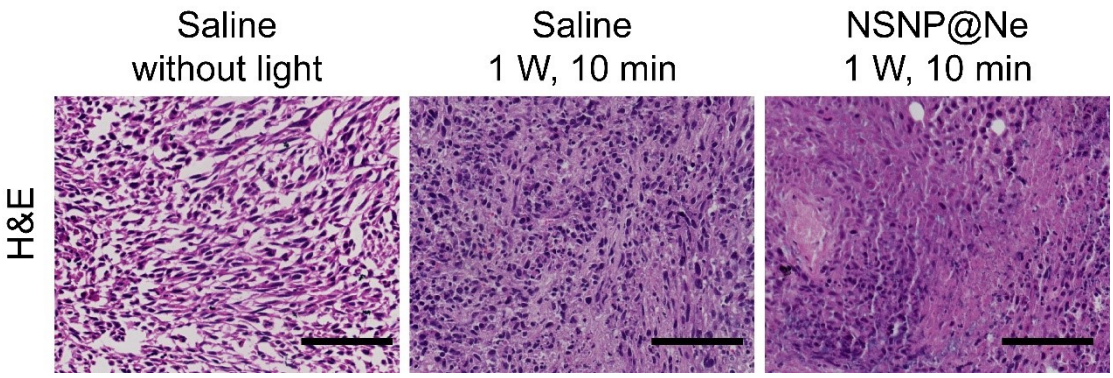

Fig. S8 Histological observation in tumor tissues stained with hematoxylin and eosin (H&E) collected from tumor-bearing mice with different treatments after 24 h. (scale bar = 100 μm).

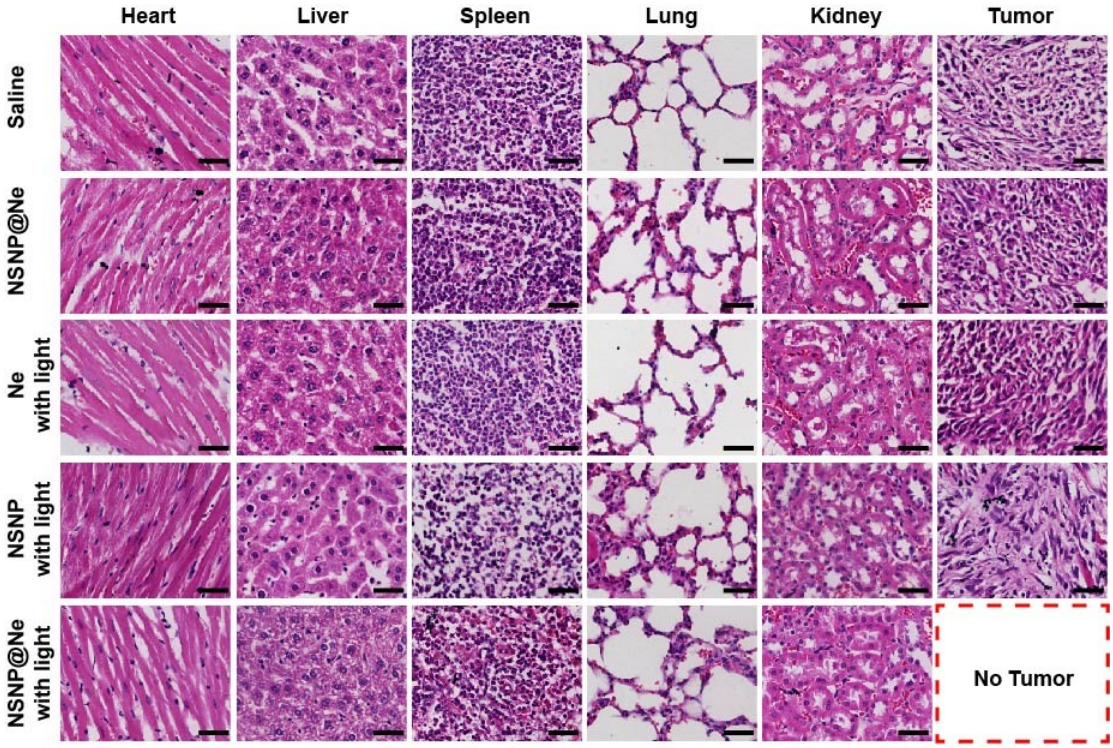

Fig. S9 Histological observation in major organs (including heart, liver, spleen, lung, kidney) and tumor stained with H&E collected from tumor-bearing mice with different treatments on 34th day (the NSNP@Ne+light group showed no tumor recurrence until the end of the experiment) (scale bar = 50 μm).

Table S1 Data for photothermal conversion efficiency.

	τ_s (s)	hS (W/˚C)	T_{max}-T_{surr} (˚C)	Q_{dis} (W)	I (W/cm^2)	A_{808}	η
NSNP	220.3	0.01907	17.50	0.002100	2	0.6351	20.27 %